LAUNCH

Victor Little **Nolan Goldthwaite** **Timothy Clifford** **Bingchen Li**

ABSTRACT

The University of Rochester Pumpkin Launch Competition is an annual event in which participants design mechanical systems to launch pumpkins at controlled distances. The objective of this project was to design and fabricate a launcher capable of winning the 2027 competition. Because scoring emphasizes both distance and accuracy, the floating arm trebuchet (FAT) was selected.

The FAT is a modernized counterweight trebuchet in which the counterweight drops vertically along a guided track rather than following a circular arc. This configuration improves energy transfer by eliminating energy losses from horizontal counterweight motion, resulting in increased launch distance. It also improves repeatability and accuracy by removing variability introduced by swinging motion. Launch performance is more predictable since the available potential energy depends only on counterweight mass and drop height.

Finite Element Analysis (FEA) was used in Siemens NX to model the trebuchet arm and ensure it could withstand repeated loading forces while achieving the target launch distance of 300 ft for a 3 lbf pumpkin. FEA was also used to evaluate the release pins and trigger mechanism, providing direction for the final pin angles and trigger geometry.

The frame was constructed primarily from 2x4 and 4x4 lumber with cross-bracing to support the load from the counterweight. A base with removable wheels was integrated to transport the frame, which weighs over 300 lb. The launcher operates by engaging a barbell counterweight via a rope-actuated release. As the counterweight falls, the arm transitions from a rear pivot to a guided rail, allowing smooth forward motion until the sling releases.

Mechanical analysis predicts launch distances of 300 ft with a 150 lbm counterweight and 50 ft with a 45 lbm counterweight. This project applied principles of structural design, energy transfer, dynamic systems, and safety in the development of a function pumpkin launcher.

PROBLEM DEFINITION

Engineering systems that store and release energy in a controlled and repeatable manner are critical across many industries. Applications such as launch systems, lifting mechanisms, and impact devices rely on predicable energy transfer, structural reliability, and safe operation under dynamic loading conditions. Designing systems that efficiently convert stored potential energy into directed motion requires careful consideration of energy transfer efficiency, structural stresses, release timing, and safety factors.

This project addresses these broader engineering challenges through the design and construction of a pumpkin launcher for the University of Rochester's annual pumpkin launch competition. This competition challenges student teams to design mechanical systems capable of launching pumpkins significant distances with accuracy, repeatability, and safe operation. The University of Rochester has not won this competition outright in six years, this opens the door for a more optimized and analytically driven design approach.

The objective of this project is to develop a high-performance launcher capable of delivering pumpkins between 50-300ft while maintaining structural integrity and consistent release behavior. The system must maximize energy transfer efficiency while ensuring that dynamic loads do not exceed allowable material stress. Achieving this balance requires integration of rotational dynamics, projectile motion modeling, stress analysis, and controlled release mechanisms.

By improving launch distance, repeatability, and reliability, this project addresses the competitive performance gap while serving as a practical application of core mechanical engineering principles. The resulting system aims not only to meet functional requirements, but to position the University of Rochester to win the pumpkin launch competition.

REQUIREMENTS, SPECIFICATIONS, DELIVERABLES

Requirements:

1. Device capable of safely, reliably, and repeatably launching a pumpkin at different target distances.
2. Launcher will be purely mechanical and not use any chemical propellants/electrical power.
3. Human power will not be used to hold the launcher in an energized state before firing.
4. The launcher will be evaluated prior to the competition.
5. Stored mechanical energy used to launch the projectile will be created with the judges who are present.
6. The launcher must be suitable for transport and setup at the launch site.

7. The launcher must maintain its integrity through multiple uses.
8. The device must follow all competition rules and site constraints.
9. The launcher must be easy and quick to assemble.

Specifications:

The specifications are based on the pumpkin launch competition requirements and mechanical analysis. According to the competition rules, since the target distances start from 50ft from the previous competition rules and are kept adding until reaching 300ft, we will use these as our minimum and maximum distances, respectfully. While measuring the launching distances, the launcher will be set and launched to the target distance and then measure the pumpkin landing point from the target distance by using a tape measure. The maximum width of the launcher is 4ft based on requirements as well, and it will be measured from tape measurement. For accuracy of the launching distance and ultimation of the launcher's setting over other launchers, mean error of the launching distance will be 5% over 3 shots, since over 50ft above the target distance will be counted as 0 points. To make the entire launcher feasible to be assembled, each part of the launcher shall be movable and carriable, since there are 4 people in the team, and it is plausible to make 2 people carry one part, each part of the launcher will be within 120lbf, and each part's weight will be verified by scale check. Meanwhile, the safety of audiences and operators is always in the first place of mechanical engineering design, and failure of the launcher will make all what the team did previously wasted. Therefore, the minimum factor of safety for yield of material is set to 2, and it will be verified with ruler and mark, and check the displacement of the marked place when the launcher is fully loaded. FEA simulation may also be applied to evaluate the designed structure before assembly. In addition to that, the fully loaded launcher is required to be stable at 15 degrees inclined, and it will be measured with a protractor. All these above are the guidelines of designing the launcher and standards to determine whether the design is successful when the launcher is assembled.

Deliverables:

1. Prototype Device (Pumpkin Launcher)
2. Technical Report
3. Theory of Operation (Instruction manual for launcher)
4. Test Data Analysis
5. Safety Plan

CONCEPTS

Multiple launch concepts were generated to address the performance requirements of the University of Rochester Pumpkin Launch Competition. Team members developed each concept independently to ensure diversity in mechanical approach and energy transfer mechanisms. Concepts were evaluated based on launch efficiency, structural feasibility, safety, controllability, manufacturability, and expected repeatability. (Table 1)

MECHANICAL ANALYSIS

The mechanical design of the Floating Arm Trebuchet was developed to achieve the project requirements of launching a 3 lbf pumpkin to a target distance range of 50-300 ft while maintaining structural integrity and safe operation. A combination of analytical calculations and CAD simulations was used to validate the design. CAD modeling, finite element analysis (FEA), and motion simulations were conducted using Siemens NX to evaluate system performance and structural behavior under loading conditions. Key subsystems analyzed include the beam, pivot/axle mechanism, counterweight assembly, and support frame. The following sections describe the analyses performed, the results obtained, and how these results directly influenced final design decisions.

A fundamental mechanical analysis was performed by modeling the trebuchet arm as a cantilever beam subjected to loading from the counterweight and projectile. A free body diagram was developed to determine reaction forces and bending moments at the pivot point, which represents the location of maximum stress. Using standard beam theory, the bending stress was calculated based on the applied moment, cross-sectional geometry, and material properties. The beam was modeled as a 4×4 cross-section, allowing for the determination of the moment of inertia and resulting stress distribution. This analysis provided an initial estimate of the maximum stress experienced during operation and was used to calculate a factor of safety relative to the material yield strength. The results confirmed that the selected beam dimensions were sufficient to withstand loading, and this analysis guided the selection of beam size and arm ratio in the final design.

Motion simulations were conducted to evaluate the dynamic performance of the trebuchet and to optimize launch parameters. A simplified skeleton model of the Floating Arm was created in NX, incorporating the translating pivot, counterweight, and sling system (Figure 1). Simulations were run with a projectile mass of 3 lbf and varying counterweight masses and release angles to achieve. Three release pin angles of 60˚, 70˚, and 80˚ were selected to evaluate their influence on launch performance across different target distances. For each configuration, key outputs include projectile velocity, angular velocity, and predicted launch distance were recorded (Table 3-5, Figure 3-8). The simulation results demonstrated that release pin angle plays a significant role in controlling launch distance.

To calculate the release angle of the projectile, the velocity components in the Y and Z directions were extracted from the NX simulation results. These components were then used to calculate the resultant launch velocity and launch angle using standard vector relationships. Thus, allowed for a more precise determination of projectile trajectory and ensured consistency between simulation outputs and analytical projectile motion equations. By resolving the velocity into components, it allowed validation of simulation results and improved

understanding of how release conditions influenced overall system performance.

The data showed that a counterweight range of 45-150lbm was sufficient to achieve the minimum and maximum distances of 50 ft and 300 ft respectively (Table 3-5). The range of configurations allowed the system to meet all performance requirements without requiring excessive increases in counterweight mass.

The relationship between release angle, counterweight mass, and resulting launch distance was analyzed. These results directly influenced the final design by establishing a multi-configuration launch strategy, where the release pin angle can be adjusted to achieve different target distances while maintaining a consistent counterweight range. This approach improves system flexibility and efficiency while minimizing structural loading associated with excessively large counterweights.

Finite element analysis (FEA) was performed to evaluate the structural integrity of the trebuchet under loading conditions. Rather than applying simplified static loads alone, a more representative loading scenario was developed by integrating results from the NX motion simulation. Specifically, data snapshots from the skeleton (mechanisms) model were extracted at discrete time steps throughout the launch cycle, capturing the dynamic forces and positions experienced by the arm during operation. These snapshots were then imported into the FEA environment within Siemens NX to create time-dependent loading conditions.

To accurately represent the free-body behavior of the trebuchet arm during motion, Inertia Relief (INREL) was utilized in place of traditional fixed boundary conditions. Since the arm is not rigidly constrained during operation and instead undergoes dynamic motion, applying standard constraints would introduce artificial reaction forces and unrealistic stress distributions. Inertia relief allows the system to be analyzed as a free body by automatically balancing applied loads with inertial forces, effectively simulating the actual operating condition of the arm as it accelerates and rotates during launch. This approach results in a more physically accurate representation of stress and deformation throughout the structure.

The model geometry of the arm was meshed using tetrahedral CTETRA (10) element formulation with refinement applied in regions expected to experience high stress, particularly neat the pivot/axle interface and along areas of geometric transition. Loads derived from the motion simulation were applied at each time step, allowing the analysis to capture the variation in force magnitude and direction throughout the launch event (Table 6).

The resulting stress contour plots identified the maximum stress occurring near the pivot region, which is consistent with the location of maximum bending moment predicted by analytical calculations (Figure 10). Deflection results indicated that deformation along the arm remains within acceptable limits and does not significantly impact launch performance (Figure 10) The peak stress values obtained from the time-stepped analysis were compared to the material yield strength, resulting in a factor of safety of approximately 2.

The use of inertia relief, combined with time-dependent loading, provided a simulation of real operating conditions. This analysis confirmed that the selected beam dimensions are structurally adequate, identified critical regions for potential reinforcement, and validated that the design withstand repeated use. Additionally, this approach demonstrates strong integration between motion simulation and structural analysis, increasing confidence in the overall mechanical design.

The pivot point of the trebuchet experiences significant radial loading due to the weight of the beam and counterweight. A bearing analysis was performed to evaluate the loads acting on the pivot and to determine appropriate sizing and material selection. Reaction forces at the pivot were calculated using static equilibrium, resulting in an estimated radial load of approximately 700 lbf, under a 200 lbf counterweight condition (Table 6), representing a conservative loading case. These forces were used to estimate the required load capacity of the bearing or axle interface. Consideration was also given to friction and wear, as these factors can impact system efficiency and longevity. Based on these requirements, a 5/8-inch diameter high-strength steel axle, commonly used in go-kart and racing applications, was selected due to its proven ability to withstand high dynamic loads and resist wear. The analysis ensured that the selected pivot design can safely support operational loads while maintaining smooth motion. This directly influenced the choice of axle diameter and material, contributing to both durability and overall system performance.

Material selection for the trebuchet arm was based on achieving a balance between strength, stiffness, weight, cost, and manufacturability. The primary structural member was constructed using laminated 3/4-inch plywood, selected for its favorable strength-to-weight ratio and availability. To characterize the effective material properties of the beam, a simply supported beam analysis was performed using measured or estimated deflection data to approximate stiffness and validate its structural performance under loading. This provided a practical, experimentally informed estimate of the material behavior for use in design calculations.

The plywood layers were oriented and bonded such that the direction of primary bending during operation is perpendicular to the face of the plywood sheets. This configuration leverages the laminated structure of plywood, where alternating grain directions improve strength and reduce the effects of anisotropy. By stacking and gluing multiple layers, the beam effectively behaves as a composite section with increased thickness and stiffness. Additionally, this orientation ensures that the outer fibers of the beam—where bending stresses are highest—are supported by multiple bonded plies, maximizing resistance to tensile and compressive stresses.

The lamination strategy also improves structural performance by increasing the moment of inertia of the cross-section and enhancing load distribution across the beam. This results in greater resistance to bending and reduced deflection compared to a single solid member of equivalent thickness. The

final laminated beam design provided sufficient strength to withstand operational loads while maintaining a low mass, contributing to improved dynamic performance of the trebuchet.

Overall, the use of laminated plywood, combined with strategic orientation and bonding, resulted in a cost-effective and structurally efficient solution that met the performance and safety requirements of the design.

A torque and preload analysis was conducted for the primary fastening element connecting the 2x4 and 4x4 wooden structural members. The connection utilizes a ½ in diameter, 6 in long carriage bolt, which is responsible for maintain clamping force and structural integrity during launcher operation.

The analysis followed standard bolted joint theory, where tightening torque is related to preload using.

$$T = KF_i d \quad (1)$$

Where T is the applied torque, K is the torque coefficient, F_i is the preload force, and d is the nominal bolt diameter. The preload was determined as 75% of the bolt proof load, which is consistent with recommendations for non-permanent connections.\

For a ½-13 UNC carriage bolt with a tensile stress area of 0.1419 in^2 and an assumed proof strength of 60 ksi (A307 grade), the proof load was calculated as 8514 lbf. This resulted in a recommended preload of approximately 6385 lbf. Using a typical torque coefficient of $K = 0.2$, the required tightening torque was found to be 53.2 ft-lbf. This value represents the target installation torque under dry conditions. In addition to bolt loading, the analysis evaluated wood bearing stress beneath the washer to assess the risk of local crushing. Using a washer outer diameter of 1.25in and a standard clearance hole, the effective bearing area was calculated as 0.979 in^2. The resulting compressive stress in the wood was approximately 6525 psi. This stress level is significantly higher than the compressive strength. Even with pressure treated lumber, with the assumptions of improved durability, the torque preload relationship for the carriage bolt remains the same.

Pressure-treated wood improves environmental durability, but it does not eliminate the risk of wood crushing from bolt preload. The connection should still use oversized washers or steel plates and avoid applying the full 53.2 ft-lbf torque unless crushing is acceptable or experimentally verified.

This influenced the design by showing that the bolt itself was not the limiting component. Instead, the pressure-treated wood around the bolt head and nut controlled the connection design. As a result, the team prioritized load-spreading hardware and practical torque control during assembly rather than simply tightening the bolt to the maximum calculated torque.

A fatigue analysis of one of the sling pins was used to evaluate if, after testing and many launches, it would deform or break. If deformation occurred, our launch distance could change, and a drift between predicted values and measured values may occur. This would lead to the prediction model to be no longer applicable. An infinite fatigue life under expected loading is ideal. The part is manufactured from ¼ inch thick AISI 1008 HR steel, with an ultimate tensile strength of 44,000 psi and a yield strength of 24,500 psi. A finite element model was constructed in NX Nastran using Tet10 elements at a mesh size of 0.249 inches, with RBE2 rigid body elements attaching the hole faces to fixed boundary condition points, constrained in all translational and rotational degrees of freedom (Figure 12). A 25 lbf load was applied perpendicular to the sling ring supporting surface, representing the sling ring traveling along the entire length of the hook shaped pin.

Nodal stress results were extracted from the simulation and used as inputs to a MATLAB fatigue analysis based on the Modified Goodman and Soderberg criteria. The endurance limit was computed using the Marin equation, yielding Se = 11,761 psi after applying surface, size, load, temperature, and reliability correction factors. From the maximum and minimum principal stresses across all nodes (1,128.43 psi and −1,136.89 psi respectively), the alternating and mean stress components were calculated as σ_a = 1,132.66 psi and σ_m = −4.23 psi. A secondary check using the von Mises stress extremes (1,878.75 psi and 0.07 psi) yielded σ_a,vm = 939.34 psi and σ_m,vm = 939.41 psi(Figure 13).

Both operating points fall well within the safe region of the Modified Goodman and Soderberg diagrams, as shown in the figures. The computed safety factors under the max principal stress criterion were nf = 10.39 (Modified Goodman) and nf = 10.40 (Soderberg), both indicating infinite fatigue life by a substantial margin. Given the low applied load relative to the part geometry and material strength, this result is expected. The analysis confirms that this sling pin design will not fail in fatigue under the specified loading conditions.

A tolerance analysis of the release assembly was conducted to verify that the release pin will reliably assemble with the mating hole while minimizing excessive clearance that could negatively impact the consistency and performance of the release mechanism. From the final release drawing, the critical feature is the through-hole used for the release pin. Which has a diameter of 0.500 +0.030 and the assumed diameter of the bolt is $D_{pin} = 0.500\ in$ (worst-case). This assumption is conservative and ensures the analysis guarantees assembly under worst-cases conditions.

A worst-case tolerance analysis was performed to evaluate assembly feasibility. This method considers the extreme limits of manufacturing variation and ensures that all produced parts will assemble properly. Clearance between the pin and hole is defined as

$$C = D_{ho} - D_{pin} \quad (2)$$

Minimum clearance occurs when the hole is smallest and the pin is largest.

$$C_{MIN} = 0.500 - 0.500 = 0.000\ in \quad (3)$$

Maximum clearance occurs when the hold is largest.

$$C_{MAX} = 0.530 - 0.500 = 0.030\ in \quad (4)$$

This confirms that the bolt will always be assembled and the clearance is controlled within a reasonable range for functionality. This tolerance is tight enough to ensure function, but not tighter than necessary due to cost implications. It provides a balanced design that guarantees assembly while significantly improving mechanical performance. This tolerance was selected as critical to function (CTF) for the release mechanism, ensuring reliable and repeatable operation of the trebuchet.

MANUFACTURING

The trebuchet base, frame, and arm are all made of pressure-treated wood. Pressure-treated wood typically has a Young's modulus of about 6–12 GPa, whereas structural steels have a modulus of approximately 200 GPa. This means that steel is about 15 to 30 times stiffer than wood (1), which explains why wood structures show significantly larger elastic deflection under the same load, meaning the trebuchet structure can withstand dynamic impact loads without brittle failure. Wood was helpful over steel because it is much lighter and easier to cut, shape, and screw together when assembling. Furthermore, wood is typically cheaper than steel or aluminum. For example, pressure-treated lumber such as a 2×4 typically costs about $1–2 per foot at Home Depot, whereas a comparable mild steel bar of similar length can cost approximately $5–10 per foot at Home Depot, indicating that wood can be roughly 3 to 5 times more economical for structural applications (2).

NX CAD drawings of each part of the trebuchet were created first. After that, they were assembled into different big parts like arm, frame and mover base to see whether each part was manufacturable. Next, they were assembled to see whether they fit with each other and whether there was a cut that needed to be fixed. When the whole assembly was confirmed, drawings of each part of the assembly were created to make the cutsheets as audiences to cut the parts.

The Trebuchet's frame is mainly made up of 2x4 inch wood bar, and they were measured and labelled into different lengths at first. And then from the inside part of the labelled cut line or the end of bars, the angles were measured and labelled based on the cutsheet (Figure 15).

The labelled bars were brought to the Rettner Workshop to cut them into various parts using the cutting machine. After different components were made, the base plywood was labelled and cut to make mover wheels able to fit in the base (Figure 16). The base mover's feet were cut from 4x4 inch bars, then the feet were installed on the cut plywood by referencing the cutsheet and labels on the plywood. When feet were placed in right position, 10 x 3-1/2 in. Tan Torx Flat-Head Wood Deck Screws were applied on the top of the plywood and installed into the long feet at the center, front and back under it. The short feet at the bottom side of the plywood were stabilized by 1/4 in. x 6 in. Exterior Washer Head Structural Wood Lag Screws, applied from the bottom of the feet to the top of the plywood (Figure 17).

After the base was completed, 4 main supporting pillars (chute) were installed on the base by screwing from the bottom of base. On vertical dimensions, 1.5-inch-wide spacers were placed between the chutes and stabilized by clamps. Then, the supporting side bars (chute support) were installed on the base with the same way, and they were connected by a piece of sheet metal on each side which side chute supports were attached to chutes, with 2 screws on each side (Figure 11). Then the vertical rail supports were installed on the inner side of the frame against the chutes, and a vertical rail support was placed and installed above it. Next, another vertical rail support was placed at the outer side of the frame, during this process, bubble level was employed to ensure the vertical rails were placed vertically and the horizontal rails were placed horizontally. Then, a 3.5x3.5 and 1.5-inch-wide spacer were installed at both ends of the horizontal supports, then, another piece of horizontal supports and vertical supports were installed throughout the same way based on the spacers. To enhance the structure, the rail cross bracings (Figure 19) were placed and installed at an inclined degree across the structure in different orientations and formed a shape of "X". For the cross bracings attached with the chute supports, they were connected through a carriage bolt to enhance the stiffness of the structure. The processes above were repeated 4 times on each 4 corner sides of the base.

The next step was to install the 2 borders of the base. 2 borders were aligned at the left and right sides of the base, and screws were installed from outside of the borders into the chutes and support bars which contacted the borders. Then, the 4 1.5-inch-thick rails were installed on each corner side of the frame. When the frame structure was finished, the trebuchet was flipped again to install wooden blocks to hold the bars for the wheels. On the center part of the bottom, the blocks were cut to fit between the central long and short legs, and 0.625-inch holes were drilled at the center on the side faces of the blocks to fit the shafts. The 10-inch wheels were placed at the inner cuts of the base so that the pressures from both sides will be balanced to reduce the risks of collapse under heavy weight. Spacers were placed between the blocks to prevent the blocks from sliding while rotating. The blocks at the center were not screwed to make it easy to take off when the trebuchet was moved to destination. After that, the pairs of 4x4x4-inch blocks were installed at the middle of the both sides of the front and back base cuts by screws from top of the base plywood to the bottom, and the holes on these blocks were not drilled through, to make the wheel bars

just fit into the blocks to save materials and save the particles of clampers. 8-inch tires were placed in the front and back cuts on the base mover. By creating different sizes of the front and back, and the central wheel, it would be easy to rotate the trebuchet. The borders were enhanced by installing the screws from the bottom of the plywood of the base into the borders above it, so that the borders would be pinned in 2 dimensions.

At the rear of the trebuchet, a 0.625-inch-hole was drilled on each side of the 2 vertical end rail supports. Then a steel bar was put through the hole with 4 flat wheels to support the falling arm while launching. On either side of the grouping of wheels 2 clamps were applied to prevent the wheels from sliding (Figure 20).

The throwing arm is made up of 5, 0.75-thick-plywood pieces. Due to its ununiform shape, the plywood was cut through CNC cutting based on the cutsheet (Figure 21). After the pieces were cut, a 1.31- inch-hole was tapped in the machine workshop on the end of the arm for the counterweight arm. Also, a 5/8-inch-hole was tapped at the pivot point of the arm to hold the bar with wheels on the rail. And then, the 5 pieces were glued together and left for 2 days until the glue was dry (Figure 22). The central hole of the throwing arm was attached to a short bar to attach 2 10 in wheels to move on the rail for the arm to rotate after releasing, and the hole on the side of the bar was attached to a 45-lbf-bar from the gym to apply and adjust the weight for different distances of launching.

3D printing was also utilized for some parts of the trebuchet system. For the clamp-pulley system which was applied on the weight bar to turn and trigger the release system. When the CAD drawing of the clamp-pulley was created, it was exported to STL file and was printed in ABS material and took about 9 hours for each clamp-pulley. After removing the support of the printed clamp-pulley with a knife, it was ready to be used (Figure 23). The pin which is on the top of the throwing arm to release the string while launching, their shapes were created by plasma cutting. A tool path was created by NX part file (Figure 24). Then, they were sanded on the filing machine, and the holes were drilled out.

Finally, a cap is placed on the top of the chutes to hold them together. Utilizing a 2x4 as a spacer they would be applied between the chutes on each side and stabilized by clamps, then the cap would be screwed to the top of the chute to fix them together.

The total cost of the entire launch system plus the mover cost $540 USD for materials (Table 1 and 2). Some parts were taken from the existing materials from the Rettner Workshop, such as small clamps for the wheels on the frame, the bars, and the wheels.

If the working costs of team members are included, the cost of working for manufacturing will be larger since the trebuchet is larger than any other project, and all the materials need to be cut into certain dimensions and shapes to assemble. The current working hours of each team member are shown in Table 7. The estimated costs of working on manufacturing together are $11,100, while the total costs of working for each team member are $26,625. The working hours conclude the time of manufacturing, cutting materials, tapping holes, plasma cutting and running the printers for printing. The working cost is under the rate of $100/hour. The development time concludes with the time of designing, CAD drawing, FEA simulation, and iterations. Development time also occupies a substantial portion of the total working time, especially for release pin, clamp-pulley, and release plate, which were modified over many times (Table 8). The total development is 109 hours, under 100$/hour, which costs $10,900.

If the part or system were to be scaled to 1000 systems, the current manufacturing process, which relies heavily on manual measurement, cutting, and assembly of wooden components, would need to be improved to reduce costs and build time to meet the requirements of mass production. Structural components can be redesigned to include more metal parts manufactured by CNC machining and plasma cutting, or 3D printed parts with stronger materials, which provide higher repeatability and faster production compared to manual processes.

The wooden components could be redesigned into modular, prefabricated panels using laser cutting. Instead of cutting individual 2×4 and 4×4 members manually, the structure could be converted into an interlocking “building block” system with pre-cut slots and tabs, allowing parts to be assembled quickly without extensive measurement or alignment. This would significantly reduce assembly time and minimize human error. Therefore, fastening methods could also be optimized by reducing the number of individual screws and replacing them with standardized fastener kits, pre-installed threaded inserts, or quick-lock mechanisms. This would streamline assembly and improve consistency across units.

The current way of printing clamp-pulley is inefficient since it takes 9 hours to print each of them. For scaling, these parts should be converted to injection-molds and fill the ABS material into the molds to make the parts, which would reduce per-unit production time and cost once tooling is established.

Overall, transitioning from manual wood-based fabrication to a combination of CNC-machined metal components, modular laser-cut wooden structures, and mass-produced mechanical parts would significantly reduce build time, and lower overall cost when scaling to 1000 systems.

TEST PLAN and RESULTS

The specifications are based on the pumpkin launch competition requirements and mechanical analysis. Some aspects these specifications highlight are safety, moveability, and accuracy. These are the guidelines and standards that determine whether the design is successful. Refer to Table 9, a checklist of specifications and if they were met.

Initially, simple screening tests were used to find the best sling length, if a secondary roller helps reduce bouncing, and using a released weight tied to the pulley string for a more controlled release force. The sling length was evaluated at 3

lengths keeping all other variables constant. Having the sling in the middle value provided the best launch angle. Video recordings of multiple launches of the same sling confirmed this observation. Video recordings were also used to understand the impact of adding a second roller, which reduced bouncing significantly. Furthermore, although there were no issues with pulling the release pulley rope by hand, a weight also worked to controllably pull on the release pulley. This may be implemented during competition to maximize consistency. After these first screening experiments, a larger experiment was used to understand the relationship between release pin angle, projectile weight, and counterweight weight.

The testing plan of the floating arm trebuchet follows a designed experiment to build a mathematical model. s. Information about the MATLAB program can be found in the TeamLaunchProgramTheoryOfOperation document. This model will then be used to adjust counterweight weight and hit the target distance accurately. To develop a predictive model for the trebuchet, an empirical data collection experiment was designed using principles of robust design. Rather than deriving throw distance analytically from physical equations or using simulation, this approach systematically varies the controllable inputs across their operating range, prompts the user to record the resulting distances, and fits a mathematical model to the observed data. This model is then used to predict optimal settings for any combination of projectile weight and target distance encountered on competition day.

Three variables govern each throw. Counterweight mass and pin angle level are control factors — they are deliberately set by the operator before each shot. Projectile weight will eventually be a noise factor — it cannot be perfectly controlled because competition projectiles vary in mass — but in testing we can control it on every run and can hold it to three levels. The response variable is the distance the projectile traveled in feet.

Due to testing space limitations, testing did not exceed 100 feet in launch distance. Counterweight varied across 6 levels, 65, 75, 85, 95, 105, and 115 lbf. This does not yet span the full operating range of the machine. Pin angle was assessed at three levels, labeled 1, 2, and 3, corresponding to equally spaced angular increments of the release pin. Projectile weight remained constant during this short-range experiment.

The original design experiment was structured as three blocks of 12 runs, one block per pin angle level. Within each block, the pin angle was changed, and the trebuchet was fired four times per projectile weight (3 levels). For each projectile weight, the four launches had increasing evenly spaced counterweight values. Run order within each block was randomized to prevent any time-dependent effects such as fatigue, wind shifts, or mechanical settling from being mistaken for counterweight effects. This blocked structure also reflects the practical reality that changing pin angle is a more involved mechanical adjustment than adding or removing counterweight plates, making it the natural outer loop of the experiment. The total designed experiment consisted of 36 runs.

Prior to each run, the counterweight was loaded to the specified mass using 5 lbf plate increments and verified. The projectile was weighed and the mass recorded on the data sheet. The trebuchet was fired, and the landing point was measured from the release point to the nearest foot. Distance, counterweight, pin angle level, and projectile weight were all recorded for every run before proceeding to the next.

Once all 36 runs were completed, the data were entered into a JMP and MATLAB script for model fitting. A second-order regression model was specified to capture the nonlinear relationship between counterweight and distance, the influence of projectile weight, and the effect of pin angle. The model takes the form:

$$D = \beta^0 + \beta^1(CW) + \beta^2(CW^2) + \beta^3(PW) + \beta^4(CW \times PW) + \alpha^2(Pin2) + \alpha^3(Pin3) \quad (5)$$

where CW is counterweight in lbf, PW is projectile weight in lbf, and Pin2 and Pin3 are indicator variables for pin angle levels 2 and 3 respectively with level 1 serving as the reference. The quadratic counterweight term allows the model to represent the diminishing returns behavior observed physically — distance may increase rapidly at low counterweights and tapers as the machine approaches its mechanical limits. The interaction term between counterweight and projectile weight captures the fact that a heavier projectile does not simply shift distance downward uniformly but does so more severely at higher counterweight settings. MATLAB's least squares solver was used to estimate all model coefficients simultaneously from the 36 data points.

With the model fitted, the MATLAB script accepts two inputs from the operator: the measured weight of the competition projectile and the desired target distance. The script evaluates the predicted distance for all 36 counterweight and pin angle combinations at the entered projectile weight, identifies the combination whose prediction falls closest to the target, and displays the recommended counterweight and pin angle level. Two diagnostic plots are also generated: one showing the predicted distance curves for all three pin angle levels as a function of counterweight at the entered projectile weight, and one showing how sensitive the predicted distance is to variation in projectile weight at the recommended settings. Together, these outputs give the operator both a firing solution and a visual understanding of how robust that solution is to any last-minute variation in projectile mass.

During the initial short-range testing, the variation in projectile distance, the variability in the system, can be observed. The 70 and 80-degree pin configurations seen in Table 10 and 11

demonstrated strong consistency and repeatability in experimental testing. Measured launch distances showed minimal variation between trails, typically differing by only a few feet. The data exhibited tight clustering, showing stable and predictable projectile trajectories.

These results closely align with simulation predictions, which indicated that higher pin angles are well-suited for short-range launches. The increased release angle associated with these configurations results in a trajectory that is less sensitive to small variations in system behavior, such as minor difference in release timing or frictional losses.

In contrast, the 60-degree pin configuration seen in Table 12 showed significantly greater variability in launch distance. Experimental results showed a widespread in measured distances, showing reduced repeatability and inconsistent projectile trajectories. While this behavior appears to differ from simulation predictions, it is consistent with the expected physical behavior of the system under constrained testing conditions. The 60-degree pin releases the projectile at a lower angle and the limited range of testing didn't allow us to confidently evaluate the pin with higher counterweights. This would provide the system with higher energy and therefore allow the sling to reach its ideal release point at our desired point.

The agreement between simulation and experimental results for the 70 and 80-degree pin configurations shows that the NX Mechanisms model accurately captures system behavior under short-range operating conditions. These configurations produced stable trajectories and consistent distance, validating the model's predictive capability.

The discrepancy seen for the 60-degree pin configuration is attributed to limitations in the testing environment rather than inaccuracies in the simulation model. Under short-range conditions, the system does not run at its full energy potential, preventing the 60-degree configuration from achieving the velocity in release conditions, sling dynamics, and frictional effects produce disproportionately large variations in measured distances.

From a modeling perspective, this highlights the importance of incorporating correction factors into predictive tools. The collected experimental data provided a foundation for calibrating the distance prediction model, allowing simulation outputs to be adjusted based on observed real-world performances.

INTELLECTUAL PROPERTY

The pumpkin launcher itself is not patentable because the floating arm trebuchet is not a novel idea. All information about the floating arm trebuchet is available on Wikipedia. There is 1 existing patent of trebuchet, the USD540414S1 – "Trebuchet" (Figure 15), which is only about the design or appearance of trebuchet, but not about the function and mechanism because it has existed for hundreds of years. Therefore, this design will not violate any currently existing patents. If this entire design wants to be patented, it may only cover its design appearance.

However, some parts on the trebuchet can be documented as patents for their unique designs. First, the clamp–pulley triggering system developed in this design may be documented for its unique mechanical features. The system integrates a clamp and pulley mechanism to control the release of the trebuchet under load. A small cut is introduced at the connected region between the clamp and pulley, which reduces interference and allows the clamp to close more easily and reliably under force. This modification improves usability and mechanical engagement, and although the individual components are standard, the specific configuration and functional improvement could be considered for intellectual property protection if sufficiently differentiated from existing mechanisms. And currently, there is not any patent that shares any similar design with it.

The release part made from plasma cutting may also be patentable for its unique ununiformed shape design, and it significantly influenced the release behavior and safety of the trebuchet before launching to ensure the weight bar is held well before release and make release easy as well. However, the fin-shaped release pin is not patentable though it has a functional design. While this feature improves manufacturability and may influence release behavior, it is unlikely to be patentable because release pins and hook mechanisms are already widely used in trebuchet systems, and the geometric variation alone may not meet the requirement of non-obviousness.

The moving base mover is also not patentable though it makes the moving parts easy to dissemble and easy to turn and move the trebuchet. Similar designs have already been widely applied in the carts of some furniture and material stores like Home Depot.

Overall, while the complete trebuchet system is not patentable due to extensive prior art, certain subsystems—particularly release sheet and the clamp–pulley triggering mechanism—may present limited opportunities for intellectual property protection.

SOCIETAL AND ENVIRONMENTAL IMPLICATIONS

The manufacturing process for the trebuchet used environmentally conscious practices by reusing materials from previous applications. The barbell and weight set were sourced from a home gym, while the wheels and nylon straps used for the sling were taken from Rettner Workshop and can be reused after launch day. The sling itself was constructed from nylon straps and a T-shirt. The primary environmental impact of the project came from the $500+ of lumber used for the frame, arm, and base. Obtaining the lumber required two trips to Home Depot by pickup truck. Although the lumber is biodegradable and has a

lower carbon footprint than concrete or steel, its overall sustainability depends on the forestry practices used in its production.

Additional energy-intensive processes included 3D printing of ¼ scale release pins of the prototype and full-scale clamps, plasma cutting steel for the final pins and trigger mechanism, and sawing lumber. The 3D printing process presented an opportunity for reduced material and energy use, as multiple design iterations were printed. Refining the initial designs could have reduced the number of prints required.

The operation of the launcher itself does not produce any direct emissions because it is purely mechanical. The launcher does not present significant ethical or safety concerns when used as intended. However, the skills developed – particularly in designing launch systems – have potential applications in defense contexts, where ethical considerations are more serious. Despite this, the scope of this project and the final product do not raise significant ethical concerns.

RECOMMENDATIONS FOR FUTURE WORK

The primary issues with this design are wheel bouncing as the arm contacts the guide rail and barbell tilt during its descent along the track. Wheel bounce reduces launch distance by dissipating kinetic energy, while barbell tilt leads to asymmetry in the arm, disrupting the projectile release.

Wheel bounce occurs due to a loss of continuous surface contact as the arm transitions from the rear pivot wheels to the guide rail wheels. The wheel bounce also introduces additional impact forces on the frame and vibration. A cam mechanism could be used to gradually engage a roller as the arm rotates, ensuring continuous contact and eliminating bounce.

The barbell tilt results from asynchronous release in the double-sided trigger mechanism. If one side releases before the other, the barbell rotates unevenly, causing the arm to tilt. This issue was partially mitigated by redesigning the trigger so that the barbell rotates off the release pins rather than relying on simultaneous pin withdrawal. The updated mechanism, which uses clamp-pulleys to rotate the barbell, should reduce tilting. However, the issue could be further addressed by constraining additional degrees of freedom using a four-bar mechanism or one-sided rail system.

ACKNOWLEDGMENTS

We appreciate the help from our sponsor Christopher Muir, and the faculties Chris Pratt, Paul Funkenbusch, Jim Alkins, Bill Mildenberger, Samantha Kriegsman.

REFERENCES

[1] ASTM A36 Steel Properties. (n.d.). *MatWeb Material Property Data*. Young's modulus ≈ 200 GPa https://en.wikipedia.org/wiki/A36_steel?utm_source

[2] Home Depot — retail pricing for pressure-treated lumber https://www.homedepot.com/p/2-in-x-4-in-x-8-ft-2-Ground-Contact-Pressure-Treated-Southern-Yellow-Pine-Lumber-106147/206970948?utm_source=chatgpt.com

APPENDIX

FIGURES

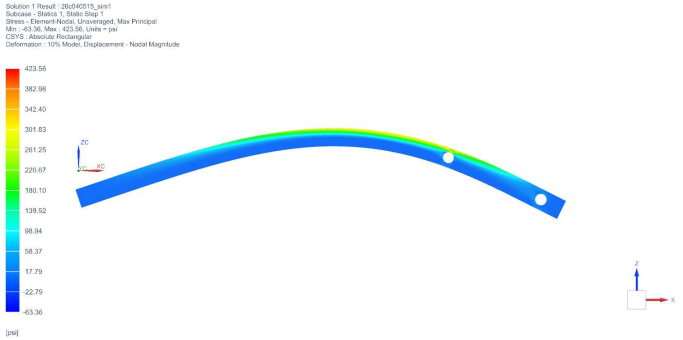

Figure 1: Initial 4x4 beam stress analysis

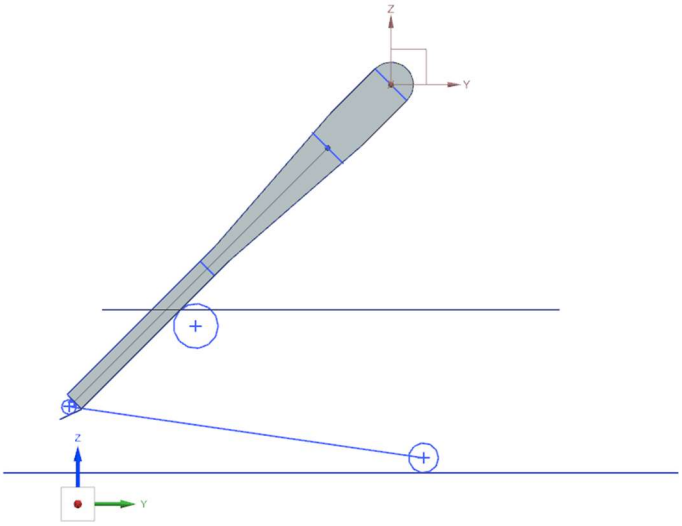

Figure 2: Skeleton model of launcher arm used for NX testing.

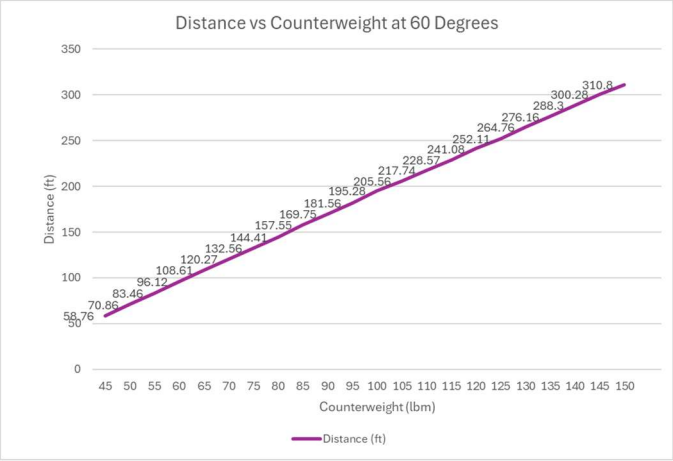

Figure 3: Counterweight to distance relationship at 60 degrees

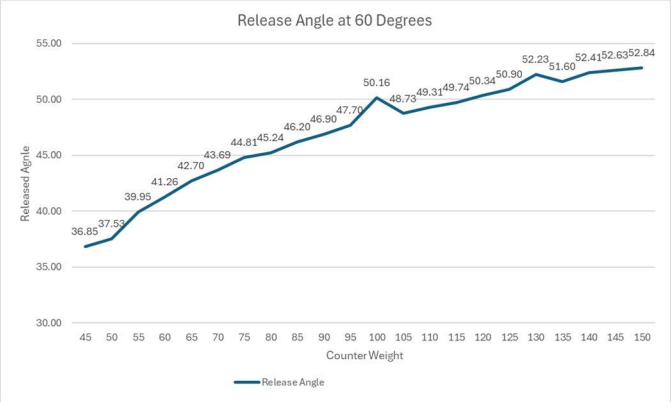

Figure 4: Counterweight to release angle at 60 degrees.

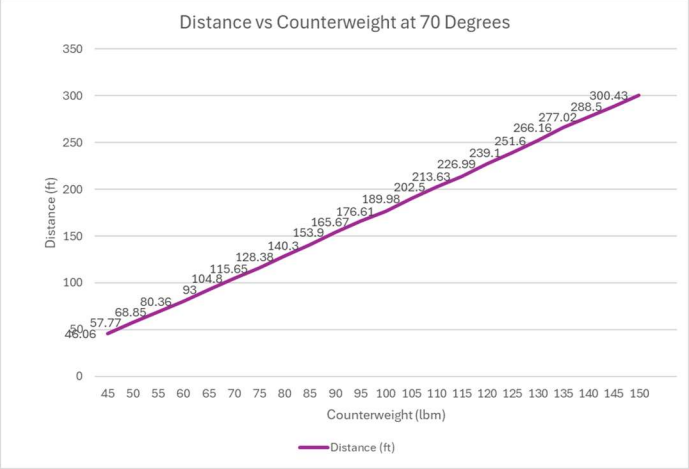

Figure 5: Counterweight to distance relationship at 70 degrees

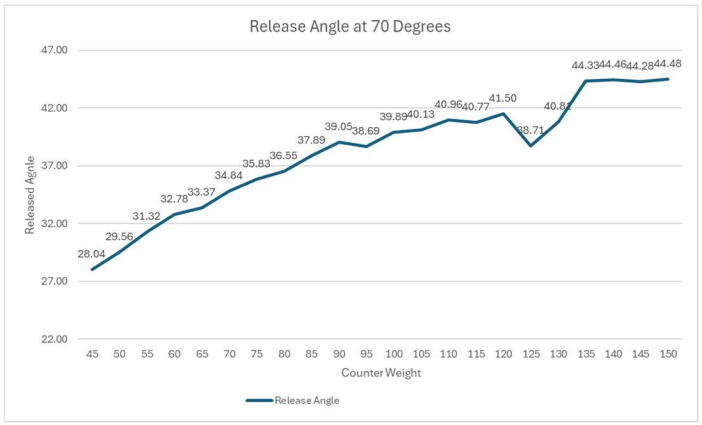

Figure 6: Counterweight to release angle at 70 degrees.

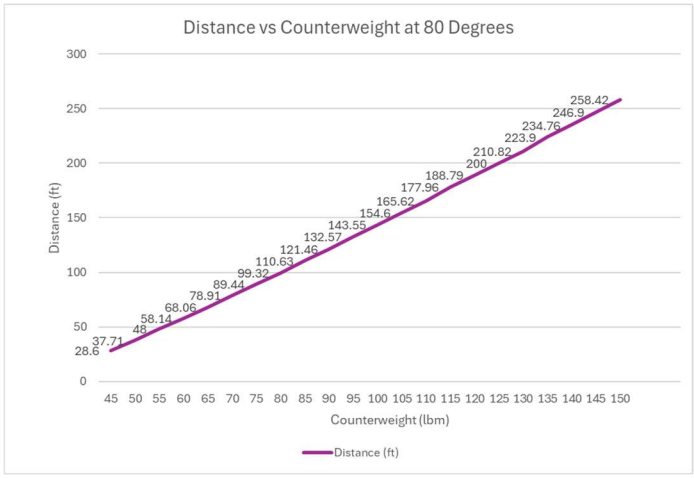

Figure 7: Counterweight to release angle at 80 degrees.

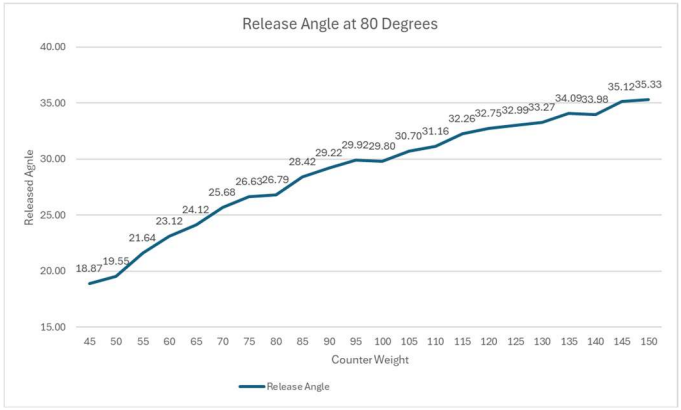

Figure 8: Counterweight to release angle at 80 degrees.

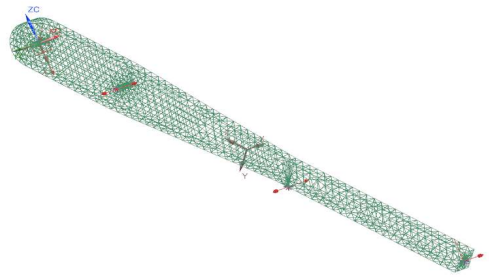

Figure 9: FEM Geometry with imported loads from skeleton model.

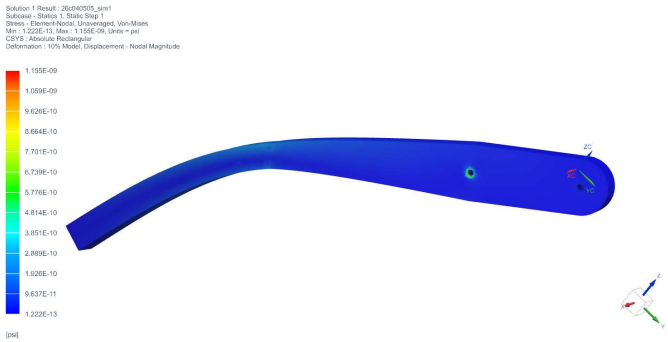

Figure 10: Von Mises Element Nodal Stress plot in psi.

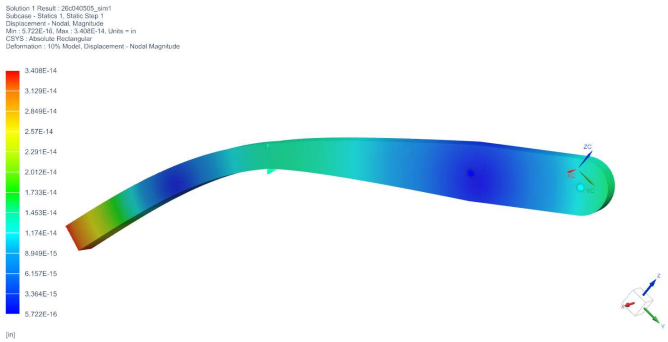

Figure 11: Displacement plot in inches of beam under loading

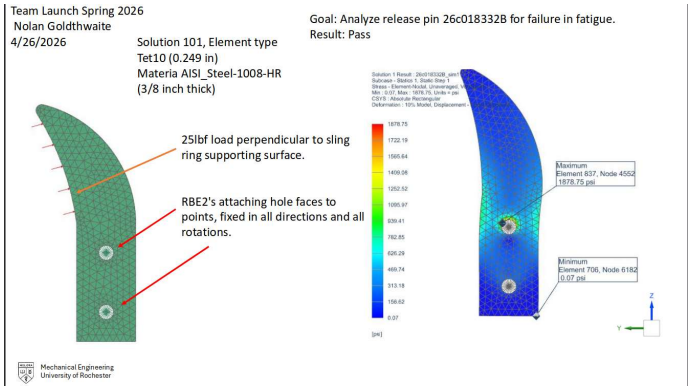

Figure 12: FEM of Sling Pin for Fatigue Analysis

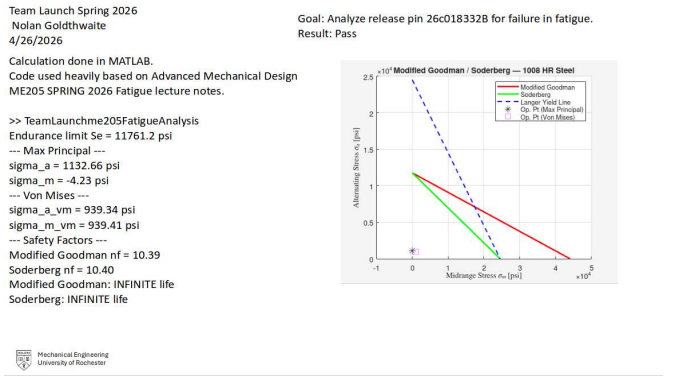

Figure 13: Fatigue Analysis and MATLAB code

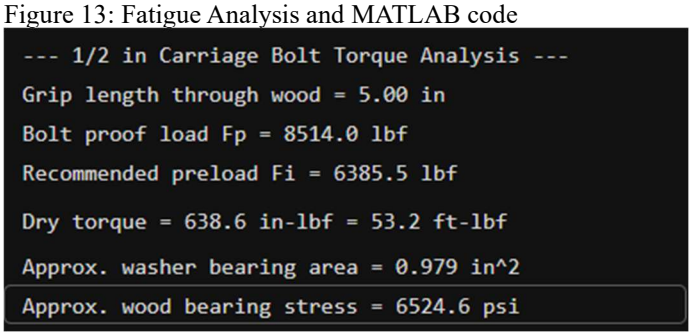

Figure 14: MATLAB results from carriage bolt torque analysis

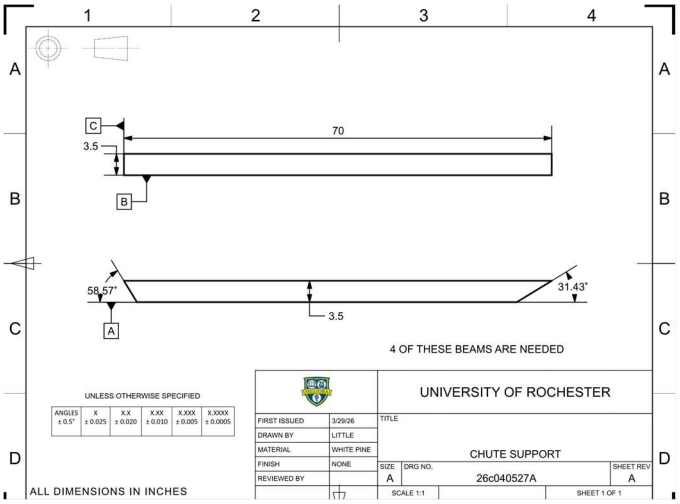

Figure 15: Cutsheet of chute support part

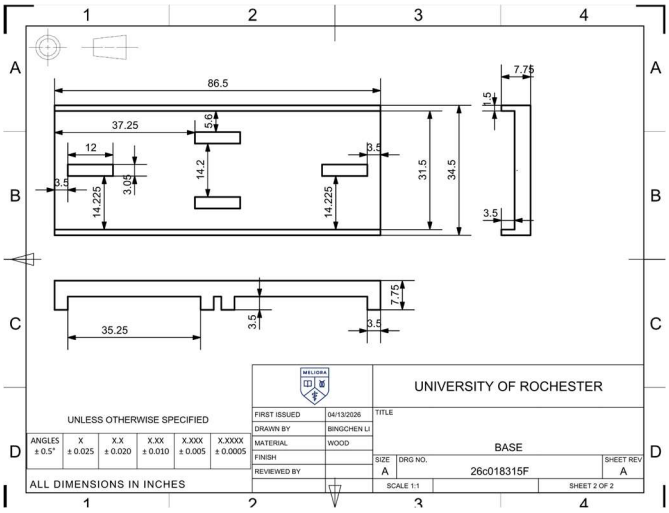

Figure 16: Cutsheet of the assembled base


Figure 17: Short feet screwed on the plywood with blocks to hold the wheels.


Figure 18: Chute with its support connected by a piece of metal sheet.

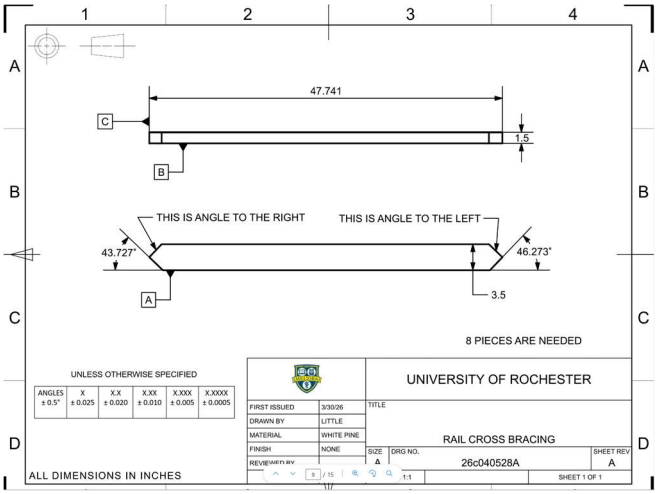

Figure 19: Cutsheet of rail cross bracing


Figure 20: Wheels support of the arm


Figure 21: Operation of Rettner Shop Bot to help cut ununiform beam geometry.


Figure 22: Trebuchet Arm glued, screwed, and let to dry with weights to limit unwanted bending.

Figure 23: A pair of printed clamp-pulley

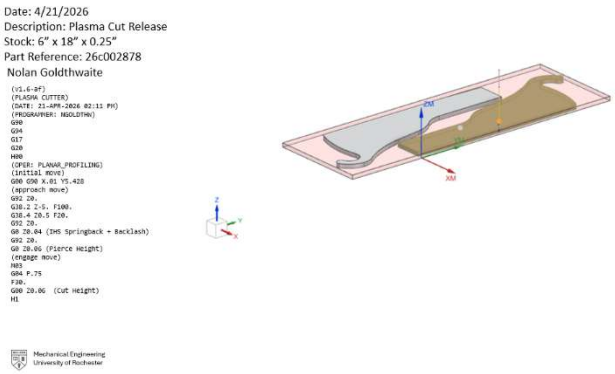

Figure 24: Plasma cutting reference of release.

Figure 25: Finished trebuchet

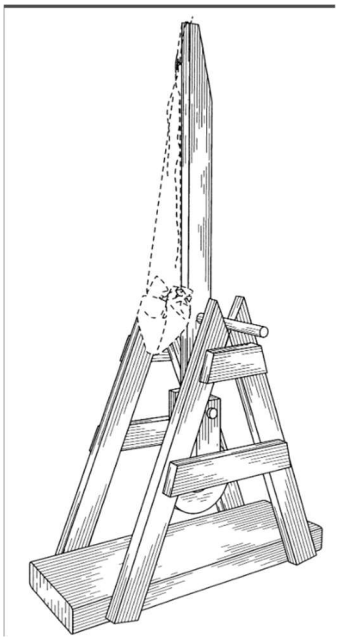

Figure 26: USD540414S1 – "Trebuchet"

TABLES

Table 1: First Round of Materials ordered from Home Depot

ID: ME205_Launcher_2604252024					
	TA/Advisor, cmuir2 and purchaser approval required				
Team	Launcher			TA/Advisor:	abermude
Contact	Chris_Muir	cmuir2@ur.rochester.edu			
Vendor	Home Depot	https://www.homedepot.com/			
Date	4/25/2026	Order Date			
Date	3/26/2026	Needed By Date			
			Total	$ 503.42	

Item	Part/Item/ASIN	Description (Add Hyperlink if possible)	Quantity	$/Each	Extended
1	329444946	2 in. x 8 in. x 8 ft. #2 Premium Grade Fir	2	$ 10.64	$ 21.28
2	206971071	3/4 in. x 4 ft. x 8 ft. Ground Contact Pressure Treated Pine	3	$ 55.18	$ 165.54
3	205220341	4 in. x 4 in. x 8 ft. #2 Ground Contact Southern Yellow Pine	10	$11.18	$ 111.80
4	206970948	2 in. x 4 in. x 8 ft. #2 Ground Contact Pressure-Treated Southern Yellow Pine	26	$ 4.58	$ 119.08
5	306587139	#10 x 3-1/2 in. Tan Torx Flat-Head Wood Deck Screw (5 lbs. / 280-Piece)	1	$ 29.97	$ 29.97
6	204633597	1/2 in.-13 x 6 in. Zinc Plated Carriage Bolt	8	$ 2.41	$ 19.28
7	315185877	1/4 in. x 6 in. Exterior Washer Head Structural Wood Lag Screws Powerlags Torx T-Star (12 Each) Bit Included	1	$ 14.47	$ 14.47
8	100375215	TP 3-1/8 in. x 7 in. 20-Gauge Galvanized Tie Plate	12	$ 1.64	$ 19.68
9	204647892	1/2 in.-13 Zinc Plated Hex Nut	8	$ 0.29	$ 2.32
10	274324	2in. X 4in. X 4ft lumber	1	$ 4.18	$ 4.18
11				$ -	
12					
13					
14					
Notes:					

Table 2: Second Round of Materials ordered from SMC Metals

ID: ME205_Launcher_2604261503					
	TA/Advisor and purchaser approval required				
Team	Launcher			TA/Advisor:	abermude
Contact	Chris_Muir	cmuir2@ur.rochester.edu			
Vendor	SMC	https://smcmetalrochester.com/			
Date	4/26/2026	Order Date			
Date	4/23/2026	Needed By Date			
			Total	$ 36.00	

Item	Part/Item/ASIN	Description (Add Hyperlink if possible)	Quantity	$/Each	Extended
1	11439	HR RECT A36 Length 16 in	1	$ 16.00	$ 16.00
2	8586	CF ROUND 1018 Length 72in	1	$ 20.00	$ 20.00
3					

Table 3: Launch distance and angle with 60̊ Pin.

Counter Weight (lbm)	Initial Y Velocity (ft/s)	Initial Z Velocity (ft/s)	Resultant Velocity (ft/s)	Launch Angle (degrees)	Pin Angle	Distance (ft)
45	26.12	34.85	43.55	36.85		58.76
50	29.27	38.1	48.05	37.53		70.86
55	32.89	39.27	51.22	39.95		83.46
60	36.06	41.11	54.68	41.26		96.12
65	39.11	42.39	57.68	42.70		108.61
70	41.98	43.95	60.78	43.69		120.27
75	44.74	45.03	63.48	44.81		132.56
80	47.43	47.03	66.79	45.24		144.41
85	50.19	48.13	69.54	46.20		157.55
90	52.94	49.54	72.50	46.90		169.75
95	55.36	50.37	74.85	47.70	60	181.56
100	60.16	50.19	78.35	50.16		195.28
105	60.19	52.82	80.08	48.73		205.56
110	62.66	53.87	82.63	49.31		217.74
115	64.57	54.68	84.61	49.74		228.57
120	67.14	55.67	87.22	50.34		241.08
125	69.27	56.3	89.26	50.90		252.11
130	72.74	56.36	92.02	52.23		264.76
135	73.72	58.42	94.06	51.60		276.16
140	76.22	58.67	96.19	52.41		288.3
145	78.24	59.76	98.45	52.63		300.28
150	79.7	60.41	100.01	52.84		310.8

Table 4: Launch distance and angle with 70° Pin.

Counter Weight (lbm)	Initial Y Velocity (ft/s)	Initial Z Velocity (ft/s)	Resultant Velocity (ft/s)	Launch Angle (degrees)	Pin Angle	Distance (ft)
45	20.01	37.57	42.57	28.04		46.06
50	22.92	40.42	46.47	29.56		57.77
55	25.84	42.47	49.71	31.32		68.85
60	28.61	44.43	52.84	32.78		80.36
65	31.19	47.35	56.70	33.37		93
70	33.89	48.68	59.32	34.84		104.8
75	36.29	50.26	61.99	35.83		115.65
80	38.7	52.2	64.98	36.55		128.38
85	41.15	52.87	67.00	37.89		140.3
90	43.73	53.91	69.42	39.05		153.9
95	45.73	57.11	73.16	38.69	70	165.67
100	47.96	57.38	74.78	39.89		176.61
105	49.97	59.28	77.53	40.13		189.98
110	52.3	60.24	79.78	40.96		202.5
115	54.09	62.73	82.83	40.77		213.63
120	56.34	63.67	85.02	41.50		226.99
125	54.44	67.93	87.05	38.71		239.1
130	58.45	67.69	89.43	40.81		251.6
135	63.17	64.66	90.40	44.33		266.16
140	64.63	65.85	92.27	44.46		277.02
145	66.21	67.9	94.84	44.28		288.5
150	67.75	68.99	96.69	44.48		300.43

Table 5: Launch distance and angle with 80° Pin.

Counter Weight (lbm)	Initial Y Velocity (ft/s)	Initial Z Velocity (ft/s)	Resultant Velocity (ft/s)	Launch Angle (degrees)	Pin Angle	Distance (ft)
45	13.11	38.35	40.53	18.87		28.6
50	15.43	43.46	46.12	19.55		37.71
55	18.04	45.48	48.93	21.64		48
60	20.39	47.75	51.92	23.12		58.14
65	22.49	50.24	55.04	24.12		68.06
70	24.83	51.64	57.30	25.68		78.91
75	26.93	53.7	60.07	26.63		89.44
80	28.65	56.75	63.57	26.79		99.32
85	30.94	57.17	65.01	28.42		110.63
90	32.92	58.86	67.44	29.22		121.46
95	34.8	60.47	69.77	29.92	80	132.57
100	36.44	63.63	73.33	29.80		143.55
105	38.47	64.79	75.35	30.70		154.6
110	40.12	66.35	77.54	31.16		165.62
115	42.22	66.9	79.11	32.26		177.96
120	43.85	68.16	81.05	32.75		188.79
125	45.51	70.1	83.58	32.99		200
130	46.87	71.44	85.44	33.27		210.82
135	49.02	72.42	87.45	34.09		223.9
140	50.36	74.73	90.11	33.98		234.76
145	52.5	74.64	91.25	35.12		246.9
150	53.87	75.99	93.15	35.33		258.42

Table 6: Force transfer from pivot roller to rail on impact

				Load analysis part=Arm				
	Arm/WeightF	Arm/WeightF	Arm/WeightF	Arm/WeightF	Arm/WeightF	Arm/LeftRoll	Arm/LeftRoll	Arm/RightRo
62	0.000	84.171	-729.776	**734.614**	**0.000**	**369.642**	**0.011**	**369.642**
63	0.000	55.494	-725.345	**727.465**	**0.000**	**365.679**	**0.015**	**365.679**
64	0.000	26.004	-704.580	**705.060**	**0.000**	**353.707**	**0.017**	**353.707**
65	0.000	-1.720	-669.570	**669.573**	**0.000**	**334.918**	**0.021**	**334.918**
66	0.000	-23.909	-631.032	**631.485**	**0.000**	**315.088**	**0.022**	**315.088**

Table 7: Total working hours and costs of working with estimated manufacturing hours and costs.

Project Hours	Tim	Levis	Victor	Nolan		
Hours for manufacturing	20	21	50	22	Manufacturing Cost $	11300
Total hours	56.75	55	109	45.5	Total Cost $	26625.00

Table 8: Development hours summary and cost

Project Hours	Tim	Levis	Nolan	Victor	Total Development Hours	Total Development Cost
Development Hours	24	27	21	37	109	10900

Table 9: Specification Pass/Fail Checklist

Specification	Test	Pass or Fail	Notes
Mean error will be less than 5% over 3 shots	Measure from the target distance line less than 5% distance to see if pumpkins have landed in range. Test conditions: clear day, sub 15 mph winds	N/A	No testing has occurred yet. See Designed Experiment section.
Launcher width no more than 4 feet	The entire launcher's width after assembly is 2 feet and 10.5 inches	Pass	
The heaviest piece must not exceed 120 lbf	All "pieces" assembled onto the launcher (arm, weight bar, weight plates) weighed less than 50 lbf.	Pass	"Piece" refers to separable components that are not on the launcher during transport.
Minimum factor of safety of 2 for yield/rupture of material	FEA analysis of launcher, arm, release mechanism.	Pass	
Device must be stable to minimum include of 15 degrees	Rolling and steering trebuchet on inclined surfaces in all directions with no tipping.	Pass	
Can hit a minimum target distance of 50ft	Set the launcher to 50ft shooting range setting, and measure the pumpkin landing point from the target distance.	N/A	No testing has occurred yet.
Can hit a maximum target distance of 300ft	Set the launcher to 300ft shooting range setting, and measure the pumpkin landing point from the target distance.	N/A	No testing has occurred yet.

Table 10: Experiment test block 70-degrees, from short range initial testing. Weight refers to counterweight; distance is in feet.

Weight	Test #	1	2	3	4	5	Average
65	Distance	52	53	53			52.66667
Weight	Test #	1	2	3	4	5	Average
75	Distance	62	63		69	62	64
Weight	Test #	1	2	3	4	5	Average
85	Distance	70	72	75			72.33333
Weight	Test #	1	2	3	4	5	Average
95	Distance	76	76	77			76.33333
Weight	Test #	1	2	3	4	5	Average
105	Distance	88	92	79	86		86.25
Weight	Test #	1	2	3	4	5	Average
115	Distance	86	89	93			89.33333

Table 11: Experiment test block 80-dergees, from short range initial testing. Weight refers to counterweight; distance is in feet.

Weight	Test #	1	2	3	4	5	Average
65	Distance	50	52	51			51
Weight	Test #	1	2	3	4	5	Average
75	Distance	62.5	63	64			63.16667
Weight	Test #	1	2	3	4	5	Average
85	Distance	73	75	76			74.66667
Weight	Test #	1	2	3	4	5	Average
95	Distance	80	78	85			81
Weight	Test #	1	2	3	4	5	Average
105	Distance	95	94	92			93.66667
Weight	Test #	1	2	3	4	5	Average
115	Distance	97	95	100			97.33333

Table 12: Experiment test block 60-dergees, from short range initial testing. Weight refers to counterweight; distance is in feet.

Weight	Test #	1	2	3	4	5	Average
65	Distance	48	40	38			42
Weight	Test #	1	2	3	4	5	Average
75	Distance	48	48	48			48
Weight	Test #	1	2	3	4	5	Average
85	Distance	52	47	52			50.33333
Weight	Test #	1	2	3	4	5	Average
95	Distance	48	61	55			54.66667
Weight	Test #	1	2	3	4	5	Average
105	Distance	73	52	62			62.33333
Weight	Test #	1	2	3	4	5	Average
115	Distance	70	62.5	75			69.16667

Appendix B – Peer Review Tracking

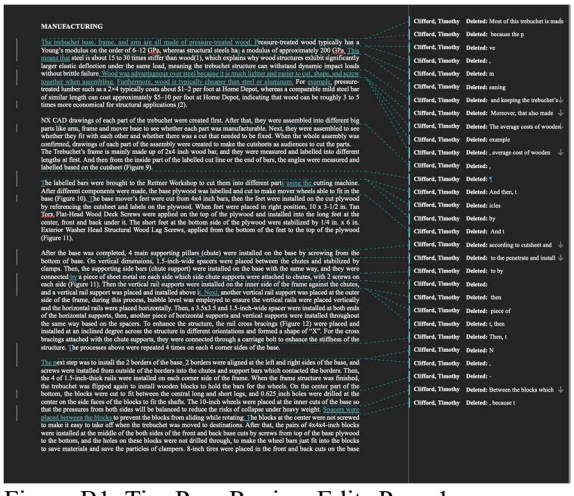

Figure B1: Tim Peer Review Edits Page 1

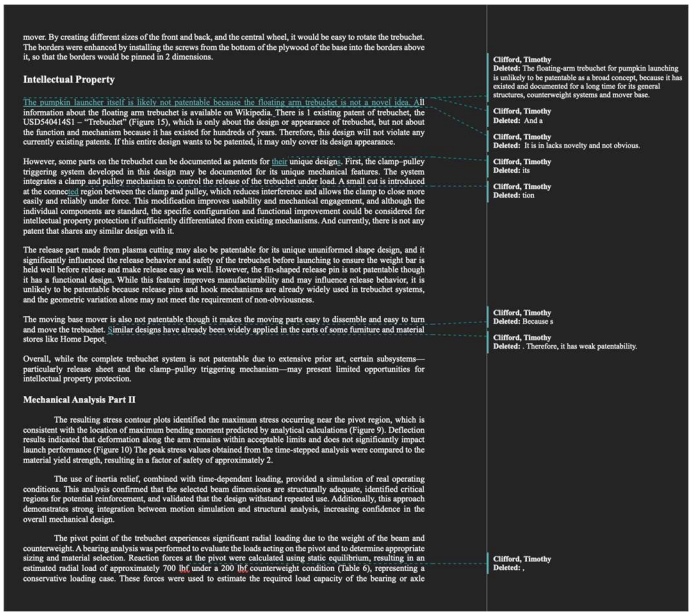

Figure B2: Tim Peer Review Edits Page 2

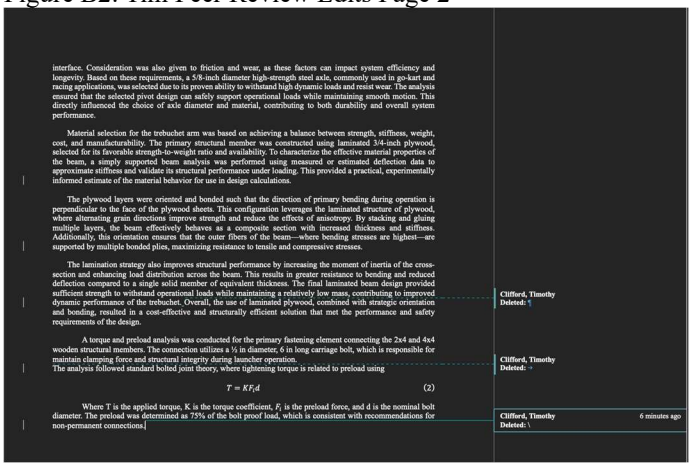

Figure B3: Tim Peer Review Edits Page 3

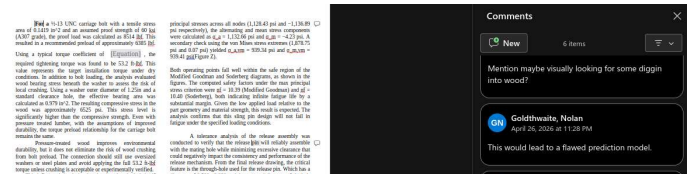

Figure B4: Nolan Peer Review Edits Page 2

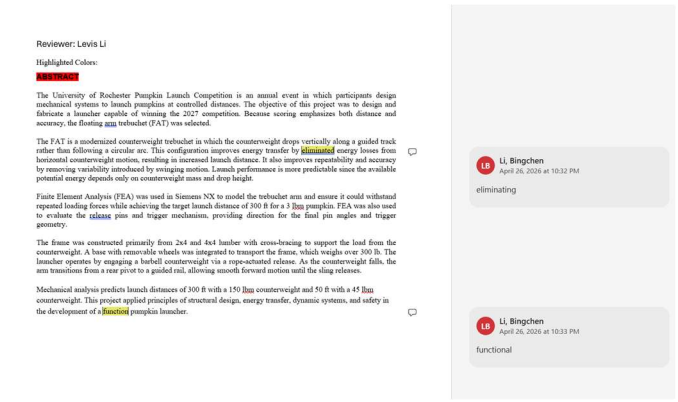

Figure B5: Levis Peer Review Edits Page 1

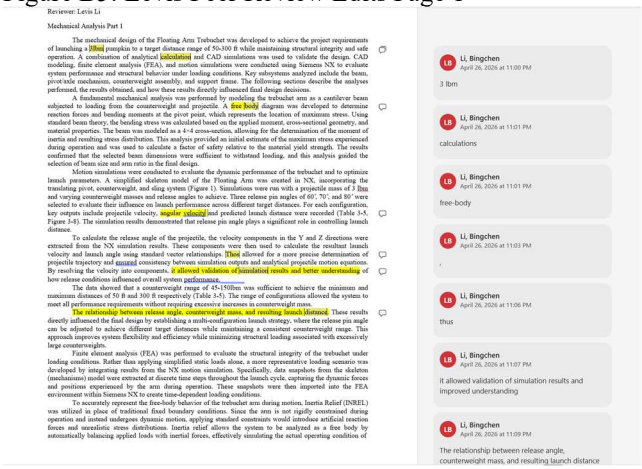

Figure B6: Levis Peer Review Edits Page 2

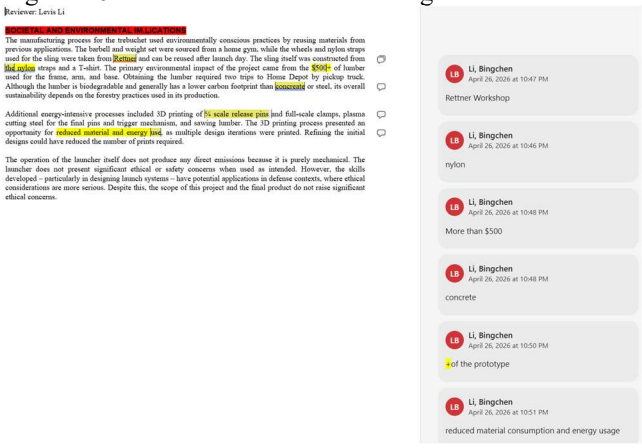

Figure B7: Levis Peer Review Edits Page 3

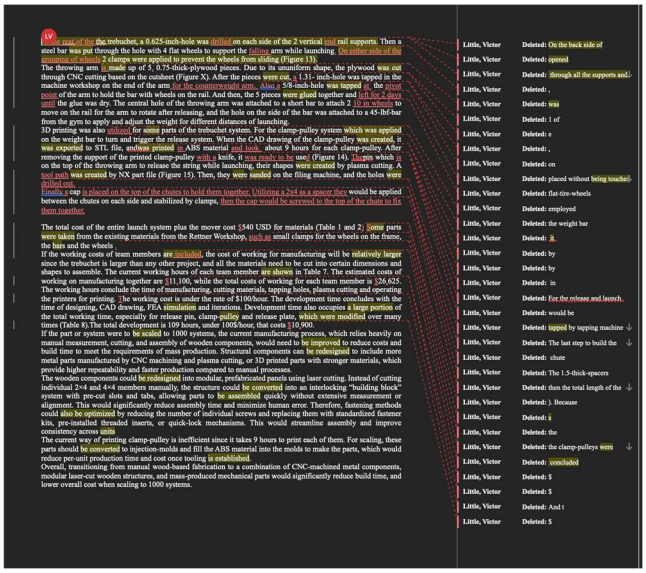

Figure B8: Victor Peer Review Edits